Bioorganic & Medicinal Chemistry Letters 21 (2011) 2264–2269

Contents lists available at ScienceDirect

Bioorganic & Medicinal Chemistry Letters

journal homepage: www.elsevier.com/locate/bmcl

Design and synthesis of isoquinolines and benzimidazoles as RAF kinase inhibitors

Hans-Peter Buchstaller *, Lars Burgdorf, Dirk Finsinger, Frank Stieber, Christian Sirrenberg, Christiane Amendt, Matthias Grell, Frank Zenke, Mireille Krier

Merck Serono, Merck KGaA, Frankfurter Straße 250, D-64293 Darmstadt, Germany

ARTICLE INFO

Article history:
Received 11 January 2011
Revised 24 February 2011
Accepted 25 February 2011
Available online 1 March 2011

Keywords:
RAF kinase
Isoquinoline
Benzimidazole

ABSTRACT

RAF kinase plays a critical role in the RAF–MEK–ERK signaling pathway and inhibitors of RAF could be of use for the treatment of various cancer types. We have designed potent RAF-1 inhibitors bearing novel bicyclic heterocycles as key structural elements for the interaction with the hinge region. In both series exploration of the SAR was focussed on the substitution of the phenyl ring, which binds to the *induced fit pocket*. Overall, it was confirmed that incorporation of lipophilic substituents was needed for potent Raf inhibition and a number of potent analogues were obtained.

The RAS-mitogen activated protein kinase (MAPK) signaling pathway, which was the first signaling pathway elucidated from the cell membrane to the nucleus,[1] has been implicated in tumor progression for a variety of human cancers. The RAF (rapidly growing fibrosarcoma[2]) kinases, which are serine/threonine kinases, are part of the MAPK signal transduction cascade: RAF—MAPK/ERK kinase (MEK)—extracellular regulated kinase (ERK). Following RAF activation in response to external stimuli such as growth factors,[3] the cascade is stimulated and MEK and ERK are sequentially phosphorylated and activated. ERK then regulates cell function by phosphorylating a variety of substrates in the cytosol and the nucleus.[4] This cascade is a vital mediator of a number of cellular fates including cell growth, differentiation, proliferation, survival, and other aspects of cellular behavior that can contribute to the transformed phenotype. All three RAF isoforms (RAF-1 or c-RAF, A-RAF, and B-RAF) are able to interact with RAS and activate the MAP kinase pathway.[5–8] In addition, it has been shown that B-RAF binds to c-RAF and activates c-RAF in a RAS-dependent manner, which reflects the complexity of the whole signaling pathway.[9–12] Activating mutations in KRAS frequently occur in various human tumors.[13] Moreover, large-scale genomic screens have also detected mutations of B-RAF in various cancer types, and therefore the RAF–MEK–ERK pathway came to the fore as possible point of therapeutic intervention in cancer.[14] A number of small molecule RAF kinase inhibitors containing diverse scaffolds have emerged in the recent past.[15,16] Beside several pan-RAF inhibitors also B-RAF selective inhibitors have been reported with strong anti-tumor activity on mutant B-RAF (V600E) tumors. However, recent studies, which show that B-RAF selective inhibitors do drive pathway activation in the presence of oncogenic RAS, highlight the importance of understanding pathway signaling in clinical practice.[9,17,18] By far the most advanced pan-RAF inhibitor, BAY43-9006, Sorafenib,[19] has been developed and launched for the treatment of renal cell carcinoma, although it has been pointed out that its activity against certain tumor types may be due to inhibition of other kinases, for example, VEGFR, rather than RAF.[20] We explored structural modifications of Sorafenib with the goal to optimize the activity on c-RAF even further. The crystal structure of Sorafenib in complex with B-RAF (PDB: 1UWH) served as a surrogate for structure-guided optimization (Fig. 1).[21,22] In this paper, we describe the design of RAF inhibitors by implementing bicyclic heterocycles as novel hinge binding motifs for this kinase.

Diverse heterocyclic groups have been used as hinge binding moieties to generate interactions with the backbone of the hinge region, for example, a pyridine in pyrazolopyrimidines[23] or a 2-carboxyamidopyridine group in Sorafenib. Azaindoles[24] or pyridoimidazolones[25] are further examples for hinge binding moieties of RAF inhibitors. A more extensive exploration of alternative hinge binders has been recently carried out by Zambon et al.[26] In our first approach we investigated the shift of the central phenyl ring of Sorafenib, which is located in the *inner hydrophobic pocket*, towards the pyridyl residue in order to gain an isoquinoline derivative. We hypothesized that this modification should retain the inhibitor in a stretched conformation and conserve the key interactions of the hinge binding part as well as the urea moiety. Moreover, we decided to keep the 2-carboxyamido group in our structures,

* Corresponding author. Tel.: +49 6151724092; fax: +49 6151723129.
E-mail address: hans-peter.buchstaller@merck.de (H.-P. Buchstaller).

0960-894X/$ - see front matter © 2011 Elsevier Ltd. All rights reserved.
doi:10.1016/j.bmcl.2011.02.108

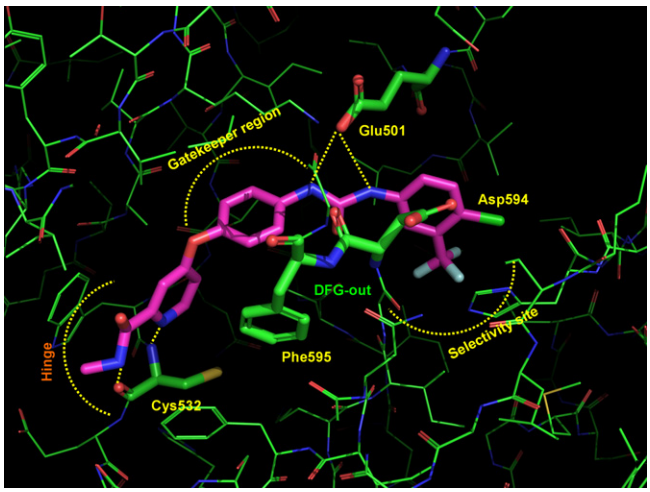

Figure 1. Crystal structure of Sorafenib (Nexavar®, BAY43-9006) bound to B-RAF kinase (PDB: 1UWH).

because we expected this residue to contribute to the binding affinity with an additional interaction to the hinge.

The prediction of the binding mode of a representative example of the isoquinoline series in complex with B-RAF, which was performed using the program GOLD,[27] is illustrated in Figure 2. Like Sorafenib the first series is thought to bind to B-RAF in a DFG-out manner.

Upon modeling, we supposed that the isoquinoline nitrogen forms a hydrogen bond with the hinge region residue Cys532 via the backbone donor and a second hydrogen bond from the carboxamide NH to Cys532 via the backbone acceptor. The urea moiety is well buried between the tight area formed by Glu501 of the αC-Helix and Asp594. Furthermore, a π-stacking interaction of the central ligand phenyl ring with Phe595 can be observed. Thus, we decided to expand our understanding of the SAR of the isoquinoline series based on this premise.

The isoquinoline analogues designed to obtain structure–activity relationships were synthesized by following the synthetic sequences summarized in Scheme 1. A key intermediate of the multi-step preparation of the isoquinoline inhibitors **10a–n** was

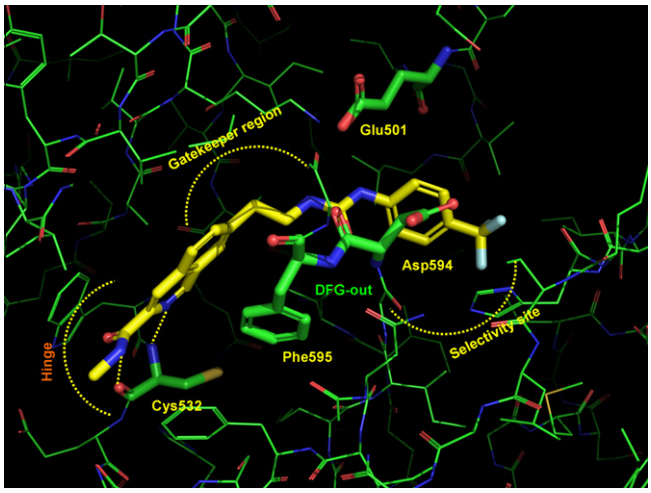

Figure 2. Model of compound **10d** docked into the active site of B-RAF. This representation depicts the extended conformation of the isoquinoline derivative, and also indicates the importance of an aromatic ring reaching out to the inner hydrophobic pocket.

compound **7**. Thus, 7-hydroxy-1,2,3,4-tetrahydro-isoquinoline-3-carboxylic acid **1a**, which was prepared according to the literature from commercially available reagents,[28] was esterified in methanol under acidic conditions to give **1b**. Oxidation of **1b** in xylene/DMF using palladium on charcoal afforded 7-hydroxy-isoquinoline-3-carboxylic acid methyl ester **2**, and the phenolic group was subsequently converted to the corresponding triflate. Attempts to gain the aldehyde **5** via Pd-catalyzed carbonylation of this species failed. For this reason, we pursued an alternative route to obtain compound **5** starting with a Stille coupling with tributylvinyl stannane to generate the vinyl substituted intermediate **3**. At this point of the reaction sequence we could either proceed with the methyl ester or the corresponding methyl amide derivative. The exploration of both pathways in parallel up to compound **6** revealed that the option to use methyl amide **4** as starting material for the following synthesis steps was superior with respect to yield and impurity profile of each of the following steps. 7-Vinyl-isoquinoline-3-carboxylic acid methyl amide **4** was prepared from the corresponding methyl ester **3** by stirring with 2 M methylamine solution in THF in presence of magnesium chloride at room temperature.[29] Subsequent osmium-catalyzed dihydroxylation of the vinyl group followed by periodate-mediated cleavage of the resulting diol afforded the aldehyde **5**. In the dihydroxylation process 1.1 equiv of *N*-methyl-morpholine-*N*-oxide (NMO) was used to regenerate OsO_4 facilitating work-up and avoiding byproducts.[30] Attempts to gain the aminoethyl-substituted isoquinoline by conversion of the aldehyde to the corresponding *O*-(ethoxycarbonyl)mandelonitrile followed by hydrogenation to the alkylamine derivative as reported by Kashdan et al.[31] was not applicable to our substrate. Thus, we obtained the desired intermediate **7** by an alternative route as follows. The acetonitrile derivative **6** was obtained from compound **5** via reduction with sodium borohydride, chlorination with thionylchloride, and nucleophilic substitution with sodium cyanide in DMSO. Finally, the nitrile **6** was quantitatively hydrogenated over Raney nickel in ethanol in the presence of ammonia to yield the key intermediate **7**.

The final isoquinoline derivatives **10a–n** were assembled using two different approaches. Hence, amine **7** was reacted with 4-chloro-3-trifluoromethyl-phenyl isocyanate **8** in dichloromethane at room temperature to produce the urea **10f**. Alternatively, the desired ureas **10a–e** and **10g–n** were obtained by consecutively treating aniline derivatives **9a–e** and **9g–n** with 4-nitrophenyl chloroformate and amine **7** in dichloromethane at room temperature in the presence of base. The syntheses of the aniline derivatives, which were not commercially available, have been reported elsewhere.[32]

The biological activities of the compounds were determined in a kinase assay.[33] Our focus of the SAR was directed towards determining the importance of the substitution pattern of the phenyl ring while maintaining the rest of the molecule intact (Table 1). It is well known from RAF inhibitors belonging to different structural families[15] that lipophilic substituents at the phenyl ring, which binds to a region called the *induced fit pocket*,[24] was needed for potent RAF kinase inhibition. Therefore, we restricted the exploration of the SAR at this position to such substituents. Assisted by our docking studies we surmised a similar elongation and orientation of this type of inhibitors like Sorafenib. This was also supported by the fact that derivatives containing a methylene bridge between the 6- or 7-position of the isoquinoline moiety and the urea unit were all inactive.[34]

We commenced our SAR effort with compound **10a** bearing a CF_3 group at the *meta* position (R^1). This derivative exhibits an IC_{50} value of about 360 nM in a c-RAF kinase assay. By replacing the CF_3 group with other lipophilic, electron withdrawing substituents—OCF_3 (**10b**) or SO_2CF_3 (**10c**)—activity could be maintained or slightly improved. However, we did not stick to the latter one due to its negative impact on the molecular weight of the compounds.

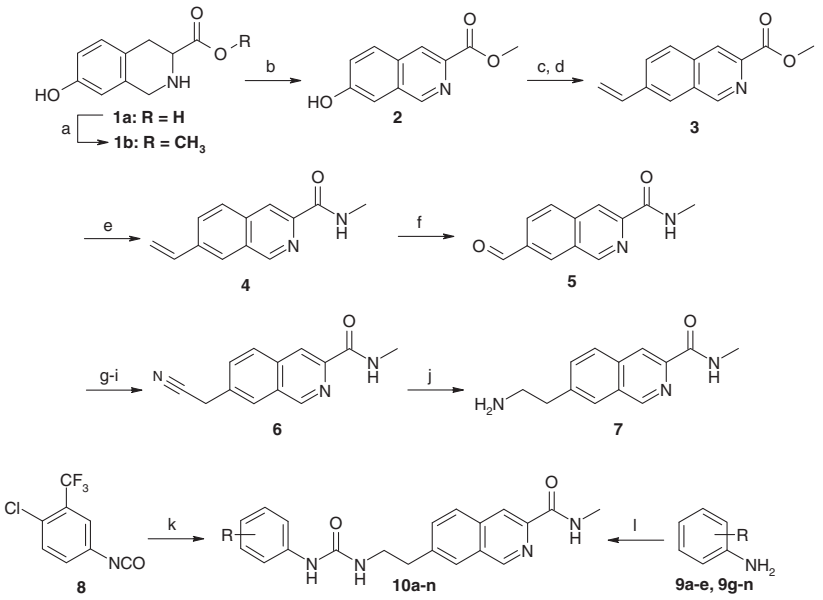

Scheme 1. Reagents and conditions: (a) H_2SO_4, MeOH, reflux, 18 h, 81%; (b) Pd-C, xylene/DMF (6:1), reflux, 3 h, 80%; (c) $(CF_3SO_2)_2$, pyridine, CH_2Cl_2, 0–5 °C, 1 h, 94%; (d) $Bu_3SnC_2H_3$, LiCl, $(PPh_3)_2PdCl_2$, DMF, 90 °C, 1 h, 67%; (e) $MeNH_2$, $MgCl_2$, THF, rt, 4 h, 81%; (f) OsO_4, $NaIO_4$, NMO, acetone/H_2O, rt, 24 h, 70%; (g) $NaBH_4$, MeOH, 81%; (h) $SOCl_2$, CH_2Cl_2, rt, 2 h, 87%; (i) NaCN, DMSO, 55 °C, 3.5 h, 57%; (j) H_2/Raney-Ni, EtOH/NH_3, 5 bar, 45 °C, 24 h, 99%; (k) **7**, CH_2Cl_2, rt, 3 h, 48%; (l) (i) *p*-NO_2PhOCOCl, pyridine, CH_2Cl_2, rt; (ii) **7**, DIPEA, rt, 23–82%.

Table 1
c-RAF inhibitory activities of isochinoline derivatives **10a–10n**

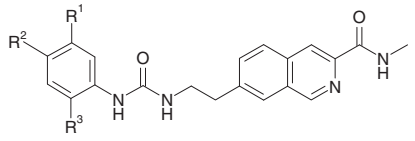

Compound	R^1	R^2	R^3	Yield (%)	c-Raf IC_{50}[a] (μM)
10a	CF_3	H	H	69	0.36
10b	OCF_3	H	H	82	0.26
10c	SO_2CF_3	H	H	59	0.20
10d	H	CF_3	H	55	0.37
10e	CF_3	CH_3	H	63	0.20
10f	CF_3	Cl	H	48	0.16
10g	CF_3	F	H	79	0.24
10h	CF_3	H	F	67	0.25
10i	CF_3	H	OCH_3	73	0.12
10j	CF_3	H	$O(CH_2)_2N(CH_3)_2$	23	0.45
10k	Cl	CH_3	OCH_3	37	0.11
10l	CH_3	Cl	OCH_3	55	0.19
10m	CF_3	Cl	OCH_3	70	0.08
10n	CF_3	Cl	$O(CH_2)_2N(CH_3)_2$	54	0.34
Sorafenib (BAY43-9006)				—	0.04

[a] c-Raf IC_{50} values were determined as described in Ref. 33.

Moving the CF_3 group from *meta* position (R^1) to the *para* position (R^2) had no impact on activity as shown by analogue **10d**. Having established the requirement of a lipophilic group like CF_3 in position R^1 of the aromatic ring, we explored the tolerance of additional substituents in other positions (R^2, R^3) as shown by analogues **10e–n**. Small residues like methyl, chloro and fluoro in position R^2 along with the CF_3 group in the R^1 position are well tolerated (**10e–g**). The introduction of a fluoro atom at this position (**10g**) was less effective than a chloro atom, or a methyl group, suggesting the importance of the substituent size. An electron donating substituent like a methoxy group (**10i**) in position R^3 was better than a fluoro atom (**10h**) improving potency compared to compound **10a** by a factor of 3. We attempted to use this position for the introduction of solubilizing residues. However, as can be seen by compound **10j** and **10n** this was not accomplished without attenuating the c-RAF inhibitory potency. The preparation of a few examples with substituents at all three discussed positions brought further insights (**10k–m**). The CF_3 group at position R^1 (**10l**) is better than a methyl group (**10m**), but also a chloro atom at R^1 with suitable residues at R^2 and R^3 yields a potent inhibitor (**10k**). This confirms that not only lipophilicity but also electronic effects contribute to the impact of substituents at this position. Compound **10m** is the most active derivative of this series exhibiting an IC_{50} value of 82 nM against c-RAF kinase, which is almost as potent as Sorafenib (IC_{50}: 40 nM) in our assay.

The docking studies suggest dividing these derivatives into two subseries based on the observed interaction patterns. Most of the isoquinoline derivatives display a similar binding mode compared to Sorafenib. However, the derivatives bearing solubilizing groups (**10j**, **10n**) do not interact with the hinge anymore, which might explain the inferior activity (Fig. 3). Some binding poses lack the optimal hydrogen bond pair between the backbone atoms of the hinge region and the ligand carboxamide atoms. As a consequence, we planned to explore reversed carboxamide for the benzimidazole series.

In our second approach we replaced the isoquinoline moiety by a substituted benzimidazole residue. This heterocycle has been exploited as hinge binder in Tie-2 and VEGFR-2 inhibitors[35] and we surmised a similar binding mode for our compounds to the hinge region of c-RAF. Similar to the isoquinoline derivatives we expected that shape and extension of the inhibitor in the binding pocket are essential for retaining the key interactions of the hinge binding part as well as the urea moiety. As for the previous series we tried to improve the potency of the compounds by exploring the SAR of the phenyl moiety. However, since solubility is a common issue of urea type inhibitors, in addition we tried to identify a position for the introduction of water solubilizing groups without affecting c-RAF inhibitory potency.

Synthetic methods for building the benzimidazole derivatives were established and are summarized in Schemes 2 and 3. Hence, for the preparation of derivatives **19a–s** two synthetic routes were

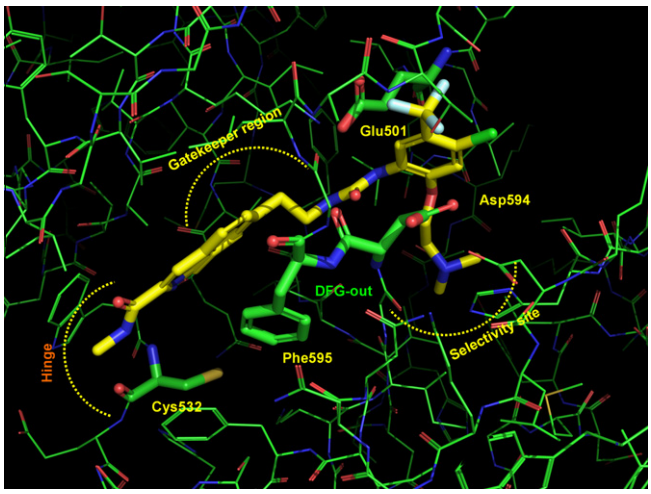

Figure 3. Predicted binding mode of compound **10n**, which lacks the protein hinge contact, but indicates gain of activity through the additional substituent.

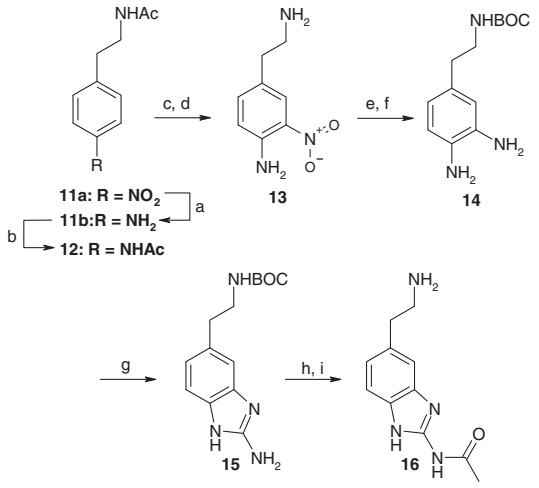

Scheme 2. Reagents and conditions: (a) H_2/Raney-Ni, MeOH, rt, 21 h, quant.; (b) Ac_2O, rt, 15 min, 92%; (c) Ac_2O, HNO_3, 0 °C, 2 h, rt, 18 h, 49%; (d) 6 N HCl, reflux, 18 h, quant.; (e) Boc_2O, NaOH, dioxane/H_2O, 0 °C to rt, 1 h, 84%; (f) H_2/Pd-C, MeOH, rt, 20 h, quant.; (g) BrCN, MeCN, H_2O/MeOH, rt, 1 h, quant.; (h) (i) AcCl, DIPEA, THF, 0 °C, 30 min, 79%; (ii) pyridine, 100 °C, 3 h, 81%; (i) CF_3COOH, CH_2Cl_2, rt, 30 min, 81%.

developed. In route I, depicted in Scheme 3 and 4-(2-aminoethyl)-2-nitro-phenylamine **13** was reacted with isocyanate **8** or aniline **9i** using the coupling conditions described for the isoquinoline series, whereas, the benzimidazole moiety bearing different functional groups was formed at a later stage. This route was used to obtain compounds **19a**,**b**,**d**,**e** allowing us to discover the most suitable substitution of the imidazole core for the interaction with the hinge region. In route II (Scheme 2 and 3), the benzimidazole ring is formed first to generate the complete hinge binding part, which could be subsequently modified to the desired urea derivatives. This second route is more suitable to quickly explore a range of different residues for the hydrophobic pocket in a parallel fashion, since there are just one or two steps, respectively, from the common intermediate to the final product. This method was adopted for the synthesis of compounds **19c**,**f–s**. However, similar to the preparation of intermediate **7**, the synthesis of building block **16** was not straightforward as outlined in Scheme 2.

The key intermediate for both synthesis routes was 4-(2-aminoethyl)-2-nitro-phenylamine **13**,[36] which was obtained from commercially available *N*-[2-(4-nitro-phenyl)-ethyl]-acetamide **11** in four steps. Hydrogenation of the nitro group over Raney nickel in methanol followed by an acetylation with acetic anhydride afforded diacetamide **12**.[36] Subsequent nitration with nitric acid in acetic anhydride and deprotection of the amino groups by refluxing in 6 N hydrochloric acid yielded 4-(2-aminoethyl)-2-nitro-phenylamine **13**.[36] The next step for the preparation of the

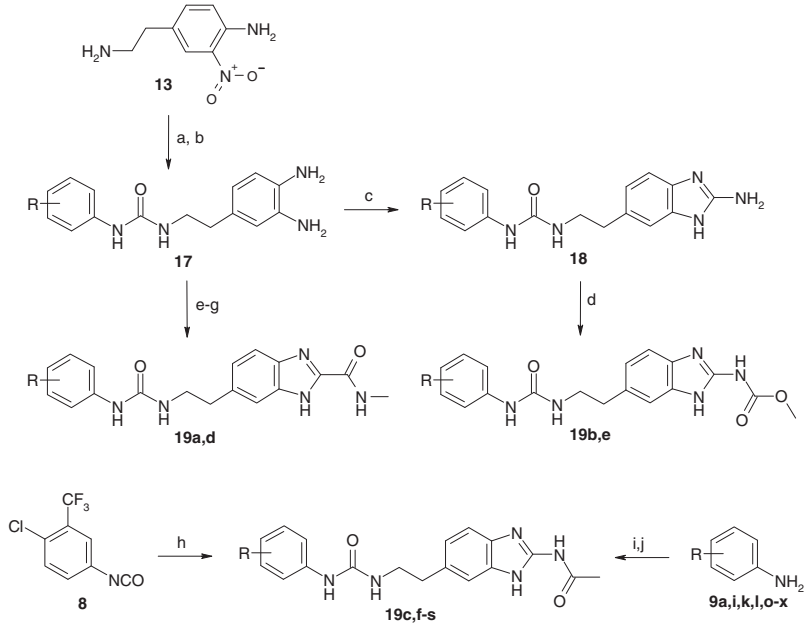

Scheme 3. Reagents and conditions: (a) **8**, CH_2Cl_2, rt, 2 h, 59%; or (i) **9i**, *p*-NO_2PhOCOCl, pyridine, CH_2Cl_2, rt, 1 h; (ii) **13**, DIPEA, rt, 30 min, 69%; (b) H_2/Raney-Ni, MeOH/THF, rt, 8 h, 82–98%; (c) BrCN, MeCN, H_2O/MeOH, rt, 3 h, 90–93%; (d) $ClCOOCH_3$, DIPEA, THF, 0 °C, 30 min, 52–57%; (e) trichloromethyl acetimidate, AcOH, 0 °C to rt, 1 h, 50–68%; (f) Na_2CO_3, MeOH/H_2O, reflux, 5 h, 77–82%; (g) $MeNH_2$, $MgCl_2$, THF, rt, 4 h, 76–98%; (h) **16**, CH_2Cl_2, rt, 3 h, 40%; (i) (i) p-NO_2PhOCOCl, pyridine, CH_2Cl_2, rt; (ii) **16**, DIPEA, rt, 19–99%; (j) CH_2Cl_2, TFA, rt, 30 min, 49–99%.

Table 2
c-RAF inhibitory activities of benzimidazole derivatives **19a–19s**

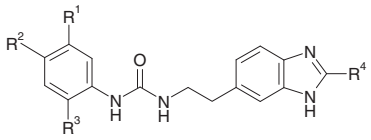

Compound	R^1	R^2	R^3	R^4	c-Raf IC_{50}[a] (μM)
19a	CF_3	H	OCH_3	$CONHCH_3$	0.34
19b	CF_3	H	OCH_3	$NHCOOCH_3$	0.81
19c	CF_3	H	OCH_3	$NHCOCH_3$	0.17
19d	CF_3	Cl	H	$CONHCH_3$	0.28
19e	CF_3	Cl	H	$NHCOOCH_3$	0.66
19f	CF_3	Cl	H	$NHCOCH_3$	0.14
19g	CF_3	H	H	$NHCOCH_3$	0.48
19h	Cl	Cl	H	$NHCOCH_3$	0.48
19i	Cl	CH_3	H	$NHCOCH_3$	0.53
19j	Cl	CH_3	OCH_3	$NHCOCH_3$	0.19
19k	CH_3	Cl	OCH_3	$NHCOCH_3$	0.32
19l	CH_3	H	$O(CH_2)_2NHCH_3$	$NHCOCH_3$	0.58
19m	CH_3	Cl	$O(CH_2)_2NHCH_3$	$NHCOCH_3$	0.49
19n	CF_3	H	$O(CH_2)_2NHCH_3$	$NHCOCH_3$	0.21
19o	CF_3	Cl	$O(CH_2)_2NHCH_3$	$NHCOCH_3$	0.23
19p	CH_3	Cl	$O(CH_2)_2NH_2$	$NHCOCH_3$	0.55
19q	CF_3	H	$O(CH_2)_2NH_2$	$NHCOCH_3$	0.25
19r	CF_3	Cl	$O(CH_2)_2NH_2$	$NHCOCH_3$	0.18
19s	CF_3	H		$NHCOCH_3$	0.23

[a] c-Raf IC_{50} values were determined as described in Ref. 33.

common intermediate **16** for synthesis route II was the protection of the aliphatic amine by reaction with di-*tert*-butylcarbonate at low temperature.[36] Diamine **14** was obtained by reduction of the nitro group with hydrogen and palladium on charcoal in methanol. For the cyclization of diamine **14** with cyanogen bromide we applied the protocol of Zou et al.,[37] yielding the 2-aminobenzimidazole derivative **15** quantitatively. In order to avoid the cleavage of the Boc-protecting group under the acetylation conditions an excess of base was added to the reaction mixture and the reaction was performed at low temperature. However, under these conditions a mixture of the *endo*- and *exo*-acetylated product was obtained as shown by NMR-spectroscopy. The product mixture was rearranged in pyridine at elevated temperature to the desired 2-acetylaminobenzimidazole derivative.[38] Removal of the Boc-protecting group under standard conditions gave rise to *N*-[5-(2-aminoethyl)-1*H*-benzoimidazol-2-yl]-acetamide **16**.

Benzimidazole derivatives **19** bearing different functional groups at the 2-position were prepared as follows (route I, Scheme 3). Urea derivatives **17** were obtained by reaction of 4-(2-aminoethyl)-2-nitro-phenylamine **13** with isocyanate **8** or aniline **9i** applying the coupling conditions used for the isoquinoline compounds **10** and subsequent hydrogenation of the nitro group. Cyclization of the diamine **17** to compound **18** was performed according to the procedure described above.[37] The carbamate derivatives **19b**,**e** were synthesized by carbamoylation of 2-aminobenzimidazole derivatives **18** with methyl chloroformate in the presence of base. To obtain 2-benzimidazolecarboxamide derivatives **19a**,**d**, diamine **17** was reacted, with trichloromethyl acetimidate in acetic acid, according to a procedure described by Louvet et al.,[39] to give the corresponding trichloromethylbenzimidazole derivatives. These intermediates were converted to the required carboxylic methyl esters in methanol in the presence of sodium carbonate.[40] Finally, treatment of the esters under conditions described for compound **4** afforded the target methyl amides **19a**,**d**.

Scheme 3 also shows the second part of route II, where the aminoalkyl substituted benzimidazole intermediate **16** was reacted with isocyanate **8** or anilines **9a**,**i**,**k**,**l**,**o–x** using the conditions described for the preparation of compounds **17** and thus generating the final ureas **19c**,**f–s**. The synthesis of the aniline derivatives, which were not commercially available, has been reported elsewhere.[41]

The biological data of this series, which are summarized in Table 2, clearly show that all derivatives exhibit a reasonable inhibitory potency against c-RAF. On this account we believe that our assumptions regarding the required length and orientation of this type of inhibitors were confirmed. As for the isoquinolines, this was supported by the observation that variation of the linker between urea and benzimidazole moiety was again detrimental for potency.[34] Comparison of derivatives **19a–f** (Table 2) bearing different residues at position R^4 of the benzimidazole part revealed that an acetylamino group provides the best activity. This residue is two times more potent than the methylamide residue, and almost five times more potent than the methyl carbamate. Thus, for all further derivatives this part of the molecule remained unchanged. Hypothetical binding orientation of **19e** (Fig. 4) suggests unfavorable interactions between ligand and protein at the hinge region, while **19f** displays apparently reasonable orientations.[27]

The SAR of the phenyl substitution is quite similar to that of the previous series. Lipophilic substituents at R^1 are needed for potent

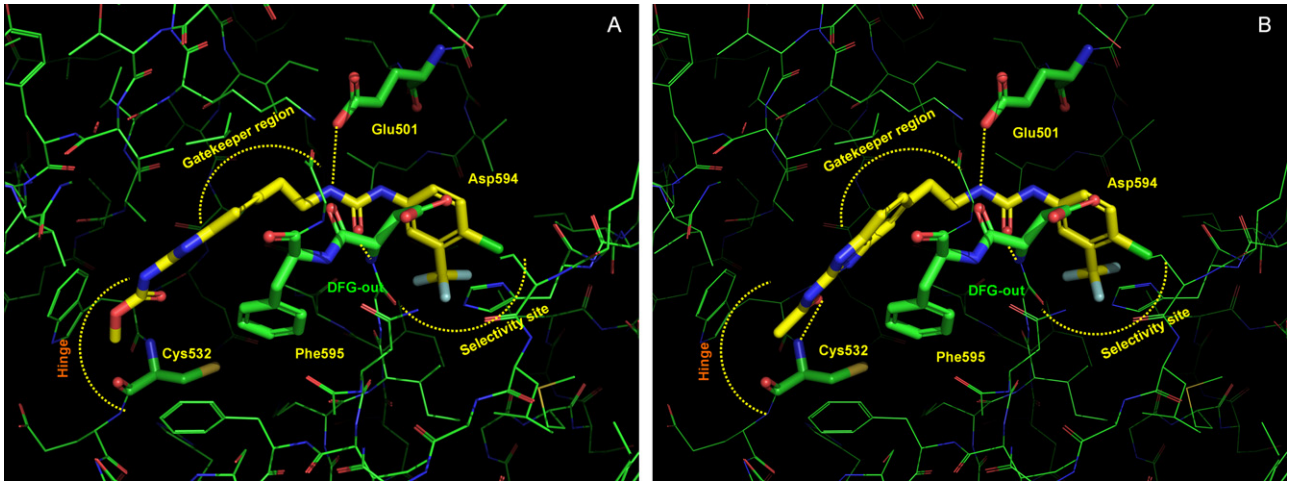

Figure 4. Predicted binding mode of compounds **19e** (A) and **19f** (B) displaying a different hinge binding behavior. Depiction of **19e** suggests unfavorable interactions, whereas depiction of **19f** illustrates favorable orientation of the hinge binding moiety.

c-RAF inhibition. Compound **19g** bearing a CF_3 group at this position exhibits an IC_{50} value of about 480 nM against c-RAF. The potency of the compounds was significantly improved by the introduction of additional substituents in other positions, for example, a chloro atom in R^2 (**19f**) or a methoxy group in R^3 (**19c**). A CF_3 group at position R^1 (**19f**) is better than a chloro atom (**19h**), but in combination with a methoxy group in R^3 potency can be regained (**19i** and **19j**). Compound **19k** is another example that proves the need for a lipophilic, electron withdrawing residue at position R^1. This methyl substituted derivative with suitable residues at R^2 and R^3 is less potent than the disubstituted derivatives **19c** or **19f**. Nevertheless, during the exploration of the SAR at position R^3 we adhered to the methyl group at R^1 due to the better physicochemical profile of the compounds. However, the lower activity of all these derivatives confirmed the need for electron withdrawing residues at position R^1. As for the first series, we used position R^3 for the introduction of solubilizing residues like aliphatic amines. Interestingly, the potency of the benzimidazoles was less affected by this modification. We assume that the loss of the acceptor hinge binding interaction is compensated by a salt bridge formed by the amine of the solubility anchor to the Asp594 side chain. Moreover, these derivatives are better soluble. For example, solubility of compound **19n** is improved by a factor of about 7 compared to compound **19c**.[42]

In conclusion, we have designed potent c-RAF inhibitors bearing novel bicyclic heterocycles as key structural elements for the interaction with the hinge region. In both series exploration of the SAR was mainly focussed on the substitution of the phenyl ring, which binds to the *induced fit pocket*. Overall, it was confirmed that incorporation of lipophilic substituents was needed for potent RAF inhibition and a number of potent analogues were obtained.

References and notes

1. Dumaz, N.; Marais, R. *Eur. J. Biol. Chem.* **2003**, *278*, 29819.
2. Wellbrock, C.; Karasarides, M.; Marais, R. *Nat. Rev. Mol. Cell Biol.* **2004**, *5*, 875.
3. Chiloeches, A.; Marais, R. In *Targets for Cancer Chemotherapy Transcription Factors and Other Nuclear Proteins*; Humana Press Inc.: Totowa, NJ, 2002; pp 179–206.
4. Kolch, W. *Biochem. J.* **2000**, *351*, 289.
5. Weber, C. K.; Slupsky, J. R.; Herrmann, C.; Schuler, M.; Rapp, U. R.; Block, C. *Oncogene* **2000**, *19*, 169.
6. Pritchard, C. A.; Samuels, M. L.; Bosch, E.; McMahon, M. *Mol. Cell. Biol.* **1995**, *15*, 6430.
7. Minamoto, T.; Mai, M.; Ronai, Z. *Cancer Detect. Prev.* **2000**, *24*, 1.
8. Yuen, S. T.; Davies, H.; Chan, T. L.; Ho, J. W.; Bignell, G. R.; Cox, C.; Stephens, P.; Edkins, S.; Tsui, W. W.; Chan, A. S.; Futreal, P. A.; Stratton, M. R.; Wooster, R.; Leung, S. Y. *Cancer Res.* **2002**, *62*, 6451.
9. Heidorn, S. J.; Milagre, C.; Whittaker, S.; Nourry, A.; Niculescu-Duvas, I.; Dhomen, N.; Hussain, J.; Reis-Filho, J. S.; Springer, C. J.; Pritchard, C.; Marais, R. *Cell* **2010**, *140*, 209.
10. Weber, C. K.; Slupsky, J. R.; Kalmes, H. A.; Rapp, U. R. *Cancer Res.* **2001**, *61*, 3595.
11. Garnett, M. J.; Rana, S.; Paterson, H.; Barford, D.; Marais, R. *Mol. Cell* **2005**, *20*, 963.
12. Rushworth, L. K.; Hindley, A. D.; O'Neill, E.; Kolch, W. *Mol. Cell. Biol.* **2006**, *26*, 2262.
13. Schubbert, S.; Shannon, K.; Bollag, G. *Nat. Rev. Cancer* **2007**, *7*, 295.
14. Garnett, M. J.; Marais, R. *Cancer Cell* **2004**, *6*, 313.
15. Khazak, V.; Astsaturov, I.; Serebriiskii, I. G.; Golemis, E. A. *Expert Opin. Ther. Targets* **2007**, *11*, 1587.
16. Li, H.-F.; Chen, Y.; Rao, S.-S.; Chen, X.-M.; Liu, H.-C.; Qin, J.-H.; Tang, W.-F.; Wang, Y.; Zhou, X.; Lu, T. *Curr. Med. Chem.* **2010**, *17*, 1618.
17. Hatzivassiliou, G.; Song, K.; Yen, I.; Brandhuber, B. J.; Anderson, D. J.; Alvarado, R.; Ludlam, M. J. C.; Stokoe, D.; Gloor, S. L.; Vigers, G.; Morales, T.; Aliagas, I.; Liu, B.; Sideris, S.; Hoeflich, K. P.; Jaiswal, B. S.; Seshagiri, S.; Koeppen, H.; Belvin, M.; Friedman, L. S.; Malek, S. *Nature* **2010**, *464*, 431.
18. Poulikakos, P. I.; Zhang, C.; Bollag, G.; Shokat, K. M.; Rosen, N. *Nature* **2010**, *464*, 427.
19. Lowinger, T. B.; Riedl, B.; Dumas, J.; Smith, R. A. *Curr. Pharm. Des.* **2002**, *8*, 2269.
20. Ramurthy, S.; Subramanian, S.; Aikawa, M.; Amiri, P.; Costales, A.; Dove, J.; Fong, S.; Jansen, J. M.; Levine, B.; Ma, S.; McBride, C. M.; Michaelian, J.; Pick, T.; Poon, D. J.; Girish, S.; Shafer, C. M.; Stuart, D.; Sung, L.; Renhowe, P. A. *J. Med. Chem.* **2008**, *51*, 7049.
21. Wan, P. T. C.; Garnett, M. J.; Roe, S. M.; Lee, S.; Niculescu-Duvaz, D.; Good, V. M.; Project, C. G.; Jones, C. M.; Marshall, C. J.; Springer, C. J.; Barford, D.; Marais, R. *Cell* **2004**, *116*, 855.
22. The structural information about the B-RAF kinase domain (SWID: P15056) is used as surrogate for the kinase domain of c-RAF (RAF1) (SWID: P04049). The residue identity is 81.7%. The hinge region has the identical sequence.
23. Gopalsamy, A.; Ciszewski, G.; Shi, M.; Berger, D.; Hu, Y.; Lee, F.; Feldberg, L.; Frommer, E.; Kim, S.; Collins, K.; Wojciechowicz, D.; Mallon, R. *Bioorg. Med. Chem. Lett.* **2009**, *19*, 6890.
24. Tang, J.; Hamajima, T.; Nakano, M.; Sato, H.; Dickerson, S. H.; Lackey, K. E. *Bioorg. Med. Chem. Lett.* **2008**, *18*, 4610.
25. Niculescu-Duvaz, D.; Gaulon, C.; Dijkstra, H. P.; Niculescu-Duvaz, I.; Zambon, A.; Ménard, D.; Suijkerbuijk, B. M. J. M.; Nourry, A.; Davies, L.; Manne, H. A.; Friedlos, F.; Ogilvie, L. M.; Hedley, D.; Whittaker, S.; Kirk, R.; Gill, A.; Taylor, R. D.; Raynaud, F. I.; Moreno-Farre, J.; Marais, R.; Springer, C. J. *J. Med. Chem.* **2009**, *52*, 2255.
26. Zambon, A.; Ménard, D.; Suijkerbuijk, B. M. J. M.; Niculescu-Duvaz, I.; Whittaker, S.; Niculescu-Duvaz, D.; Nourry, A.; Davies, L.; Manne, H. A.; Lopes, F.; Preece, N.; Hedley, D.; Ogilvie, L. M.; Kirk, R.; Marais, R.; Springer, C. J. *J. Med. Chem.* **2010**, *53*, 5639.
27. CCDC GOLD version 4.1 with default screening parameters and without any constraints. The binding mode was validated by the successful reproduction of the crystal structure via redocking, which is considered as validation for the docking of similar structures.
28. Verschueren, K.; Toth, G.; Tourwé, D.; Lebl, M.; Van Binst, G.; Hruby, V. *Synthesis* **1992**, 458.
29. Guo, Z.; Dowdy, E. D.; Li, W.-S.; Polniaszek, R.; Delaney, E. *Tetrahedron Lett.* **2001**, *42*, 1843.
30. VanRheenen, V.; Kelly, R. C.; Cha, D. Y. *Tetrahedron Lett.* **1976**, *17*, 1973.
31. Kashdan, D. S.; Schwartz, J. A.; Rapoport, H. *J. Org. Chem.* **1982**, *47*, 2638.
32. Buchstaller, H.-P.; Burgdorf, L.; Finsinger, D.; Amendt, C.; Grell, M.; Sirrenberg, C.; Zenke, F. PCT Int. Appl., WO2005/082858. *Chem. Abstr.* **2005**, *143*, 286297.
33. In a final reaction volume of 25 μL, human c-RAF (5–10 mU, Millipore) was incubated with 25 mM Tris pH 7.5, 0.02 mM EGTA, 0.66 mg/mL myelin basic protein, 10 mM Mg acetate and [γ-33P-ATP] (specific activity approx. 500 cpm/pmol). The reaction was initiated by the addition of the MgATP mix. After incubation for 40 min at room temperature, the reaction was stopped by the addition of 3% phosphoric acid solution. The reaction was then spotted onto a P30 filtermat and washed prior to drying and scintillation counting. All measurements were performed in duplicates.
34. Unpublished results.
35. Hasegawa, M.; Nishigaki, N.; Washio, Y.; Kano, K.; Harris, P. A.; Sato, H.; Mori, I.; West, R. I.; Shibahara, M.; Toyoda, H.; Wang, L.; Nolte, R. T.; Veal, J. M.; Cheung, M. *J. Med. Chem.* **2007**, *50*, 4453.
36. Kostic, S.; Soskic, V.; Joksimovic, J. *Arzneim. Forsch.* **1994**, *44*, 697.
37. Zou, R.; Drach, J. C.; Townsend, L. B. *J. Med. Chem.* **1997**, *40*, 802.
38. Graubaum, H.; Martin, D.; Csunderlik, C.; Glatt, H.-H.; Bacaloglu, R.; Malurea-Munteanu, M. *Z. Chem.* **1984**, *24*, 57.
39. Louvet, P.; Lallement, G.; Pernot-Marino, I.; Luu-Duc, C.; Blanchet, G. *Eur. J. Med. Chem.* **1993**, *28*, 71.
40. Garuti, L.; Roberti, M.; Gentilomi, G. *Farmaco* **2000**, *55*, 35.
41. Buchstaller, H.-P.; Burgdorf, L.; Stieber, F.; Amendt, C.; Grell, M.; Sirrenberg, C.; Zenke, F. PCT Int. Appl., WO2005/082862. *Chem. Abstr.* **2005**, *143*, 266924.
42. Kinetic solubility of the compounds was determined according to Hoelke, B.; Gieringer, S.; Arlt, M.; Saal, C. *Anal. Chem.* **2009**, *81*, 3165 (HPLC method) using phosphate buffer (50 mM). **10f**: 4.2 μg/ml; **10m**: <1 μg/ml; **10n**: 16.4 μg/ml; **19c**: 12.4 μg/ml; **19n**: 82.7 μg/ml; **19q**: 81.2 μg/ml.